

# ACTA TECHNICA

**Volume 58 (2013), Number 4**

ISSN 0001-7043



**Institute of Thermomechanics AS CR, v.v.i.**

# OFFPRINT

Acta Technica

<http://journal.it.cas.cz>

e-mail: [journal@it.cas.cz](mailto:journal@it.cas.cz)

© 2013 Institute of Thermomechanics AS CR, v. v. i.

Dolejšková 5, 182 00 Praha 8, Czech republic

<http://www.it.cas.cz>

ISSN 0001-7043

MK ČR E4662

# Analysis and interpretation of compressible fluid interaction upon the vibration of a circular membrane<sup>1</sup>

DANIEL G. GORMAN<sup>2</sup>, JAROMÍR HORÁČEK<sup>3</sup>,  
ANTHONY J. MULHOLLAND<sup>4</sup>, MAIRE N. GORMAN<sup>5</sup>

**Abstract.** The free vibration of a circular membrane in interaction with a fluid contained in a cylindrical boundary is analysed. The fluid is compressible and assumed inviscid. The resulting modal parameters are described by non-dimensionalised frequencies, mode shape coefficients and relative modal energy levels between that of the membrane and the fluid. A simplified “bar” model is introduced as a means of describing the characteristics of membrane/fluid strong interaction between axisymmetric modes of the membrane and axial modes of the fluid column only.

**Key words.** Vibration, membrane, fluid-structure-acoustic interaction.

## 1. Introduction

The influence of a fluid interface upon the vibration of a light flexible structure has been a subject of growing interest, particularly due to the increased deployment of thin-walled liquid/gas containers to the point where in certain cases the

---

<sup>1</sup>The research was supported by the Czech Science Foundation by project No. P101/11/0207 “Coupled problems of fluid and solid mechanics - nonlinear aeroelasticity”.

<sup>2</sup>Department of Mechanical and Aerospace Engineering, University of Strathclyde, Glasgow G1 1XQ, United Kingdom

<sup>3</sup>Institute of Thermomechanics, Academy of Sciences of the Czech Republic, 18200 Praha 8, Czech Republic; e-mail: [jaromirh@it.cas.cz](mailto:jaromirh@it.cas.cz)

<sup>4</sup>Department of Mathematics and Statistics, University of Strathclyde, Glasgow G1 1XQ, United Kingdom

<sup>5</sup>Department of Physics and Astronomy, University College London, London WC1E 6EA, United Kingdom

structural elements resemble membranes in contact with fluid. The general analysis of acoustic/structural vibration interaction problems was presented in [1], [2], where infinite series solutions for the acoustic pressure and the displacement of the structure were derived from a fundamental solution of the uncoupled problems, viz. vibration of the structure *in vacuo*, and acoustic resonance in a closed cavity with undeformable walls. These basic models were extended and applied to problems involving rectangular plates backed by rectangular cavities [3]–[6]. With respect to circular plates there has been much research reported relating to various configurations and restrictions. Lee and Singh [7] analysed the characteristics of the acoustic radiation emitted from a vibrating circular plate in free space (travelling waves) and Gorman et al. [8] considered the case of a circular disc covering a totally enclosed cylindrical acoustic cavity (standing waves) and in a subsequent publication [9] extended this analysis to introducing a method for extracting structural modal parameters from the fluid/structural interacting modal parameters. Bauer and Chiba [10] considered the case of a circular plate backed by a cylindrical cavity containing fluid assumed to be viscous and incompressible, and Amabili et al. [11], [12] considered the effect of depth of incompressible liquid upon the free vibration of circular and annular plates. With respect to circular membranes in contact with fluid, a study has been performed by Rajalingham et al. [13] to the case of a circular membrane vibrating in contact with a gas contained in an open cylindrical cavity (travelling waves) with the application to an Indian drum and Tariverdilo et al. [14] presented a comprehensive paper describing an investigation of the vibration of a circular membrane covering a totally enclosed cylindrical cavity containing *incompressible and inviscid* fluid.

This paper commences by applying the method described in [8] to obtaining the modal characteristics of a circular membrane in interaction with a closed cavity containing a *compressible and inviscid* fluid. The aim of the paper is to then extend the analysis to investigate and describe the important physical aspects which govern the degree of membrane/fluid interaction as described by relative modal energy. A simple bar model is introduced which is used to help illustrate, under certain conditions, the relationship between the natural modal roots of the coupled system and the relative modal energy of each component of the coupled system thus enabling us to consider more closely situations where there is strong structural/fluid vibration interaction.

## 2. Vibration analysis of the membrane-fluid coupled system

### 2.1 Basic analysis

The equation of motion, describing the free small lateral vibration  $w = w(\bar{r}, \theta, t)$  of a stretched circular membrane [15] in interaction with an acoustic

cavity, as shown in Fig. 1, is

$$\rho_c h a^2 \frac{\partial^2 \bar{w}}{\partial t^2} - N \nabla^2 \bar{w} = f a \tag{1}$$

where

$$\nabla^2 = \frac{\partial^2}{\partial \bar{r}^2} + \frac{1}{\bar{r}} \frac{\partial}{\partial \bar{r}} + \frac{1}{\bar{r}^2} \frac{\partial^2}{\partial \theta^2}, \quad \bar{w} = \frac{w}{a}, \quad \bar{r} = \frac{r}{a},$$

$N$  is the constant inplane force intensity,  $\rho_c$  is the membrane mass density,  $a$  and  $h$  are the radius and thickness of the membrane, respectively, and  $f$  is the acoustic pressure inside at the interface between the fluid and the membrane.

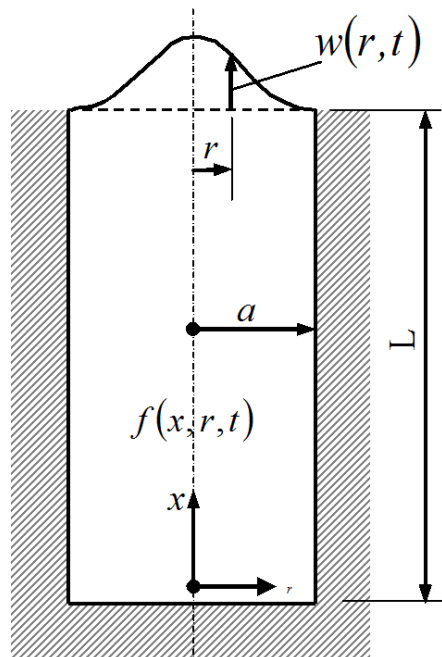


Fig. 1. Scheme of membrane/fluid interacting system

The boundary conditions in terms of  $(\bar{r}, \theta, t)$  are

$$\bar{w}(1, \theta, t) = 0, \quad |\bar{w}(0, \theta, t)| < \infty.$$

Now writing

$$\bar{w}_m = \sum_{s=1}^{\infty} \chi_{m,s} \psi_{m,s}(\bar{r}) \cos(m\theta) e^{i\omega t} \quad \text{for } m = 0, 1, \dots, \tag{2}$$

where  $\psi_{m,s}(\bar{r})$  is the natural mode shape of the membrane in the absence of fluid interaction and  $\chi_{m,s}$  is a constant for that mode, generally referred to as the *mode shape coefficient* for the mode comprising  $m$  nodal diameters

(or angular half waves) and  $s$  nodal circles. In this particular case, for a circular membrane supported at the periphery, the mode shapes  $\psi_{m,s}(\bar{r})$  are, according to [16],

$$\psi_{m,s}(\bar{r}) = J_m(\xi_{m,s}\bar{r})$$

where  $\xi_{m,s}$  are roots (values for  $s = 1, 2, \dots$ ) computed from the equation which describes the lateral displacement of the membrane at the periphery to be zero for all time:

$$J_m(\xi_{m,s}) = 0 .$$

For particular values of  $m$  and  $s$ , the natural frequency of free undamped vibration  $\omega_{m,s}$  is then

$$\omega_{m,s} = \frac{\xi_{m,s}}{a} \sqrt{\frac{N}{\rho_c h}} = \frac{\xi_{m,s}}{a} c_c$$

where  $c_c = \sqrt{N/(\rho_c h)}$ . Listed below are values of  $\xi_{m,s}$  for modes of a circular membrane clamped around the periphery characterised by  $m$  nodal diameters and  $s$  nodal circles:

$s$	$\xi_{0,s}$	$\xi_{1,s}$	$\xi_{2,s}$	$\xi_{3,s}$
1	2.4048	3.8317	5.1356	6.3807
2	5.5201	7.1056	8.4172	9.7210
3	8.6537	10.1735	11.6198	13.0152

where  $s = 1$  represents the node at the peripheral boundary.

For a particular mode of vibration for the membrane in the absence of fluid interaction, substitute (2) into (1) with  $f = 0$ :

$$N \nabla^2 [\psi_{m,s}(\bar{r})] \cos(m\theta) = -\omega_{m,s}^2 \rho_c h a^2 \psi_{m,s}(\bar{r}) \cos(m\theta) . \tag{3}$$

Therefore combination of Eqs. (1), (2) and (3) for a fixed value of  $m$  gives

$$\sum_{s=1}^{\infty} [(\omega_{m,s}^2 - \omega^2) \chi_{m,s} \psi_{m,s}(\bar{r})] \cos(m\theta) e^{i\omega t} = \frac{f}{\rho_c h a} . \tag{4}$$

The form of the acoustic pressure  $f$  acting on the membrane will now be established by reference to the acoustic cavity. Consider the acoustic cavity shown in Fig. 1, whose velocity potential  $\bar{\varphi} = \bar{\varphi}(\bar{x}, \bar{r}, \theta, t)$  is described (see, e.g., [1], [2]) by

$$\frac{\partial^2 \bar{\varphi}}{\partial \bar{r}^2} + \frac{1}{\bar{r}} \frac{\partial \bar{\varphi}}{\partial \bar{r}} + \left(\frac{a}{L}\right)^2 \frac{\partial^2 \bar{\varphi}}{\partial \bar{x}^2} + \frac{1}{\bar{r}^2} \frac{\partial^2 \bar{\varphi}}{\partial \theta^2} = \left(\frac{a}{c_f}\right)^2 \frac{\partial^2 \bar{\varphi}}{\partial t^2} \tag{5}$$

where  $\bar{\varphi} = \varphi/(ac_f)$  and  $\bar{x} = x/L$ ,  $c_f$  is speed of sound in the cavity and  $L$  is the depth of the cylindrical cavity. The boundary conditions are

$$\frac{\partial \bar{\varphi}}{\partial \bar{r}}(1, \bar{x}, \theta, t) = 0, \quad \frac{\partial \bar{\varphi}}{\partial \bar{x}}(\bar{r}, 0, \theta, t) = 0, \quad \bar{\varphi}(0, \bar{x}, \theta, t) < \infty.$$

Now writing for a selected value of  $m$

$$\bar{\varphi}_m = H_m(\bar{x}) \cdot Q_m(\bar{r}) \cos(m\theta) e^{i\omega t} \tag{6}$$

and substituting (6) into (5) gives

$$\left(\frac{a}{L}\right)^2 \frac{H_m''}{H_m} = - \left[ \frac{Q_m''}{Q_m} + \frac{1}{\bar{r}} \frac{Q_m'}{Q_m} - \frac{m^2}{\bar{r}^2} + \left(\frac{\omega a}{c_f}\right)^2 \right] = \pm k^2 \tag{7}$$

where  $k$  is a constant. The case where the right hand side of (7) is equal to  $-k^2$  (harmonic solution) gives

$$Q_m(\bar{r}) = BJ_m(\alpha\bar{r}) + \tilde{B}Y_m(\alpha\bar{r})$$

where  $\alpha = \sqrt{(\omega a/c_f)^2 - k^2}$  or  $k = \sqrt{(\omega a/c_f)^2 - \alpha^2}$  and  $\tilde{B} = 0$  since  $Q(\bar{r})$  must be finite when  $\bar{r} \rightarrow 0$ . At  $\bar{r} = 1$

$$\frac{\partial \bar{\varphi}_m}{\partial \bar{r}} \Big|_{\bar{r}=1} \equiv \frac{dQ_m}{d\bar{r}} \Big|_{\bar{r}=1} = 0. \tag{8}$$

Therefore for a selected value of  $m$ , Eq. (8) has roots  $\alpha_{m,q}$  ( $q = 1, 2, \dots$ ), which satisfy the equation  $J'_m(\alpha_{m,q}) = 0$ . Listed below are values of  $\alpha_{m,q}$  which satisfy this condition. Note that  $q = 1$  represents the node at the peripheral boundary.

$q$	$\alpha_{0,q}$	$\alpha_{1,q}$	$\alpha_{2,q}$	$\alpha_{3,q}$
1	0	1.8412	3.0542	4.2012
2	3.8317	5.3314	6.7061	8.0152
3	7.0156	8.5363	9.9695	11.3459

Since

$$\frac{dH_m}{d\bar{x}} \Big|_{\bar{x}=0} = 0, \quad H_m = C \cos(\gamma_{m,q}^{(\lambda)} \bar{x})$$

where  $\gamma_{m,q}^{(\lambda)} = \sqrt{\lambda^2 - \bar{\alpha}_{m,q}^2}$ ,  $\lambda = \omega L/c_f$  and  $\bar{\alpha}_{m,q} = \bar{L}\alpha_{m,q}$ ,  $\bar{L} = L/a$ , Equation (6) for a fixed value of  $m$  now becomes

$$\bar{\varphi}_m = \sum_{q=1}^{\infty} B_{m,q} \cos(\gamma_{m,q}^{(\lambda)} \bar{x}) J_m(\alpha_{m,q} \bar{r}) \cos(m\theta) e^{i\omega t}. \tag{9}$$

At  $\bar{x} = 1$ , the axial component of the velocity of the gas and the lateral velocity of the membrane must be equal, i.e.,

$$\frac{c_f}{L} \frac{\partial \bar{\varphi}}{\partial \bar{x}} \Big|_{\bar{x}=1} = \frac{\partial \bar{w}}{\partial t} \quad \text{for } 0 \leq \bar{r} \leq 1 .$$

Therefore combining (2) and (9) renders

$$-\frac{c_f}{L} \sum_{q=1}^{\infty} \left[ B_{m,q} \gamma_{m,q}^{(\lambda)} \sin \gamma_{m,q}^{(\lambda)} J_m(\alpha_{m,q} \bar{r}) \right] = i\omega \sum_{s=1}^{\infty} \chi_{m,s} \psi_{m,s}(\bar{r}) . \quad (10)$$

Now using the orthogonal properties of the eigenfunction  $\bar{r} J_m(\alpha_{m,q} \bar{r})$  by multiplying both sides of (10) by  $\bar{r} J_m(\alpha_{m,q} \bar{r})$  and integrating between  $0 \leq \bar{r} \leq 1$  according to [17] gives

$$B_{m,q} = \frac{-2i\omega L}{c_f} \frac{\sum_{s=1}^{\infty} \chi_{m,s} k_{m,qs}}{\gamma_{m,q}^{(\lambda)} \sin \gamma_{m,q}^{(\lambda)} \left( 1 - \frac{m^2}{\alpha_{m,q}^2} \right) J_m^2(\alpha_{m,q})} \quad (11)$$

where for a fixed value of  $m$

$$k_{m,qs} = \int_0^1 \bar{r} \psi_{m,s}(\bar{r}) J_m(\alpha_{m,q} \bar{r}) \, d\bar{r} ,$$

the value of which can be obtained through standard numerical integration.

Now the pressure  $f$  at the surface of the membrane is given by

$$f = -\rho_f a c_f \frac{\partial \bar{\varphi}}{\partial t} \Big|_{\bar{x}=1}$$

where  $\rho_f$  is the fluid density. Therefore combining (9) and (11) renders

$$f = -2\omega^2 a L \rho_f \sum_{s=1}^{\infty} \sum_{q=1}^{\infty} \frac{\chi_{m,s} k_{m,qs} J_m(\alpha_{m,q} \bar{r})}{\gamma_{m,q}^{(\lambda)} \tan \gamma_{m,q}^{(\lambda)} \left( 1 - \frac{m^2}{\alpha_{m,q}^2} \right) J_m^2(\alpha_{m,q})} \cos(m\theta) e^{i\omega t} . \quad (12)$$

Substituting (12) into (4) gives

$$\begin{aligned} & \sum_{s=1}^{\infty} (\omega_{m,s}^2 - \omega^2) \chi_{m,s} \psi_{m,s}(\bar{r}) = \\ & = -2\omega^2 \frac{\rho_f L}{\rho_c h} \sum_{s=1}^{\infty} \sum_{q=1}^{\infty} \frac{\chi_{m,s} k_{m,qs} J_m(\alpha_{m,q} \bar{r})}{\gamma_{m,q}^{(\lambda)} \tan \gamma_{m,q}^{(\lambda)} \left( 1 - \frac{m^2}{\alpha_{m,q}^2} \right) J_m^2(\alpha_{m,q})} . \end{aligned}$$

Multiplying both sides by  $\bar{r}J_m(\alpha_{m,q}\bar{r})$  and integrating between  $0 \leq \bar{r} \leq 1$  renders

$$\sum_{s=1}^{\infty} \chi_{m,s} k_{m,qs} \left\{ \omega_{m,s}^2 - \omega^2 \left[ 1 - \frac{1}{\beta \gamma_{m,q}^{(\lambda)} \tan \gamma_{m,q}^{(\lambda)}} \right] \right\} = 0, \quad q = 1, 2, \dots, n \quad (13)$$

where

$$\beta = \frac{\rho_c h}{\rho_f L} = \frac{\text{mass of membrane}}{\text{mass of fluid in cavity}}.$$

Now, re-introducing  $\lambda = \omega L / c_f$  and  $\lambda_{m,s} = \omega_{m,s} L / c_f = \xi_{m,s} (c_c / c_f) \bar{L}$  where  $c_c = \sqrt{N / (\rho_c h)}$ ,  $c_f = \sqrt{\gamma p_0 / \rho_f}$ ,  $\gamma$  is adiabatic index ( $\gamma = 1.4$  for air),  $p_0$  is mean pressure of the fluid inside the cavity and  $\rho_f$  is fluid density, then  $\lambda_{m,s}^2 = \xi_{m,s}^2 \kappa / \beta$  where  $\kappa = N \bar{L} / (\gamma p_0 a)$  and

$$\xi_{m,s}^2 \kappa = \frac{\text{lateral stiffness of the membrane}}{\text{axial stiffness of fluid in cavity}}$$

for designated values of  $m$  and  $s$ .

Therefore after multiplying (13) by  $\beta / \omega^2$  and after some substitutions and rearrangements, Eq. (13) can now be re-written as

$$\sum_{s=1}^{\infty} \chi_{m,s} k_{m,qs} \left\{ \frac{\xi_{m,s}^2 \kappa}{\lambda^2} + \frac{1}{\gamma_{m,q}^{(\lambda)} \tan \gamma_{m,q}^{(\lambda)}} - \beta \right\} = 0, \quad q = 1, 2, \dots, n. \quad (14)$$

For a fixed value of  $m$ , Eq. (14) can be expressed in matrix form as

$$\begin{bmatrix} a_{m,11} & a_{m,12} & \cdots & a_{m,1n} \\ a_{m,21} & a_{m,22} & \cdots & a_{m,2n} \\ \vdots & \vdots & & \vdots \\ \cdots & \cdots & a_{m,qs} & \cdots \\ \vdots & \vdots & & \vdots \\ a_{m,n1} & a_{m,n2} & \cdots & a_{m,nn} \end{bmatrix} \begin{bmatrix} \chi_{m,1} \\ \chi_{m,2} \\ \vdots \\ \chi_{m,s} \\ \vdots \\ \chi_{m,n} \end{bmatrix} = \begin{bmatrix} 0 \\ 0 \\ \vdots \\ 0 \\ \vdots \\ 0 \end{bmatrix},$$

i.e.

$$\mathbf{A}\boldsymbol{\chi} = \mathbf{0}, \quad (15)$$

where  $a_{m,qs} = k_{m,qs} \bar{a}_{m,qs}$  and

$$\bar{a}_{m,qs} = \frac{\xi_{m,s}^2 \kappa}{\lambda^2} + \frac{1}{\gamma_{m,q}^{(\lambda)} \tan \gamma_{m,q}^{(\lambda)}} - \beta.$$

Equation (15) can be written in the form

$$\mathbf{A}\boldsymbol{\chi} = \left[ \frac{\kappa}{\lambda^2} \mathbf{K}\boldsymbol{\Omega} + \boldsymbol{\Theta}\mathbf{K} - \beta\mathbf{I}\mathbf{K} \right] \boldsymbol{\chi} = \mathbf{0} \quad (16)$$

where

$$\mathbf{K} = \begin{bmatrix} k_{m,11} & k_{m,12} & \cdots & k_{m,1n} \\ k_{m,21} & k_{m,22} & \cdots & k_{m,2n} \\ \vdots & \vdots & & \vdots \\ \cdots & \cdots & k_{m,qs} & \cdots \\ \vdots & \vdots & & \vdots \\ k_{m,n1} & k_{m,n2} & \cdots & k_{m,nn} \end{bmatrix},$$

$k_{m,qs} = \int_0^1 \bar{r} \psi_{m,s}(\bar{r}) J_m(\alpha_{m,q} \bar{r}) d\bar{r}$  as before,  $\mathbf{I}$  is unity diagonal matrix,

$$\boldsymbol{\Theta} = \begin{bmatrix} \Theta_{m,1} & 0 & \cdots & 0 & \cdots & 0 \\ 0 & \Theta_{m,2} & \cdots & 0 & \cdots & 0 \\ \vdots & \vdots & \ddots & \vdots & \vdots & \vdots \\ 0 & 0 & \cdots & \Theta_{m,q} & \cdots & 0 \\ \vdots & \vdots & \vdots & \vdots & \ddots & \vdots \\ 0 & 0 & \cdots & 0 & \cdots & \Theta_{m,n} \end{bmatrix}$$

where  $\Theta_{m,i} = \frac{1}{\gamma_{m,i}^{(\lambda)} \tan \gamma_{m,i}^{(\lambda)}}$  and

$$\boldsymbol{\Omega} = \begin{bmatrix} k_{m,1}^2 & 0 & \cdots & 0 & \cdots & 0 \\ 0 & k_{m,2}^2 & \cdots & 0 & \cdots & 0 \\ \vdots & \vdots & \ddots & \vdots & \vdots & \vdots \\ 0 & 0 & \cdots & k_{m,q}^2 & \cdots & 0 \\ \vdots & \vdots & \vdots & \vdots & \ddots & \vdots \\ 0 & 0 & \cdots & 0 & \cdots & k_{m,n}^2 \end{bmatrix}.$$

Now multiplying (16) throughout by  $\mathbf{K}^{-1}$  renders

$$\mathbf{K}^{-1} \mathbf{A}\boldsymbol{\chi} = \left[ \mathbf{B} + \frac{\kappa}{\lambda^2} \boldsymbol{\Omega} - \beta\mathbf{I} \right] \boldsymbol{\chi} = \mathbf{0} \quad (17)$$

where  $\mathbf{B} = \mathbf{K}^{-1} \boldsymbol{\Theta} \mathbf{K}$ .

Values of  $\lambda$  can be obtained (iterated upon) which renders the determinant of matrix  $\mathbf{A}$  equal to zero. Consequently for each of these values (roots) of  $\lambda$  the corresponding values of mode shape coefficients  $\chi_{m,1}, \chi_{m,2}, \dots, \chi_{m,s}, \dots, \chi_{m,n}$

can be obtained. The determinant of this matrix equation is obtained by performing the  $LU$  decomposition [17], whereupon the value of the determinant is the product of the diagonal terms. Subsequently these root values of  $\lambda$  which render the determinant zero are substituted back into (17) to obtain the corresponding values of the mode shape coefficients  $\chi_{m,s}$  (normalized to  $\chi_{m,1}$  in the first instance and then to the largest value) that describe which structural modes are present and dominate. The numerical convergence characteristics of (17) are described in Appendix. From (14) it can be seen that the natural roots  $\lambda$  are determined by the factors  $\kappa$  (stiffness ratio),  $\beta$  (mass ratio) and  $\bar{L}$  (geometric aspect ratio).

**2.2 Comparison with the results obtained by Tariverdilo et al.**

Tariverdilo et al. [14] developed a variational method to compute the natural frequencies of a circular membrane in contact with fluid contained in a cylindrical boundary similar to this study. However, these authors considered an incompressible fluid whereupon Eq. (5) is replaced by the Laplace equation

$$\frac{\partial^2 \bar{\varphi}}{\partial \bar{r}^2} + \frac{1}{\bar{r}} \frac{\partial \bar{\varphi}}{\partial \bar{r}} + \left(\frac{a}{L}\right)^2 \frac{\partial^2 \bar{\varphi}}{\partial \bar{x}^2} + \frac{1}{\bar{r}^2} \frac{\partial^2 \bar{\varphi}}{\partial \theta^2} = 0$$

and they only reported results for the asymmetric modes of vibration ( $m \neq 0$ ). The physical parameters and dimensions were  $a = L = 60$  mm,  $h = 0.5$  mm,  $N = 100$  N/m,  $\rho_c = 2700$  kg/m<sup>3</sup> and  $\rho_f = 1000$  kg/m<sup>3</sup>. By assuming the fluid to be water ( $\rho_f = 1000$  kg/m<sup>3</sup>), we therefore selected the speed of sound waves in the fluid  $c_f = 1466$  m/s. Therefore from the relationships listed between Eqs. (13) and (14) we arrive at  $\kappa = 0.775 \times 10^{-6}$  and  $\beta = 0.0225$ . Accordingly Table 1 compares a selection of frequency values ( $c_f \lambda / (2\pi L)$  [Hz]) obtained from the variational method of Tariverdilo et al. [14] and the analysis described in this study.

Table 1. Comparison of frequency values (Hz) obtained by the present study, with those obtained by Tariverdilo et al. [14]

$m, s$	Tariverdilo et al.	Present study
1, 1	19.150	19.433
1, 2	52.895	53.897
1, 3	94.598	92.501
2, 1	32.730	34.234
2, 2	70.797	69.987
2, 3	115.681	112.970
3, 1	46.668	46.586
3, 2	88.911	88.048
3, 3	136.788	134.020

The results of Table 1 demonstrate reasonably good agreement between frequency values obtained using the two methods bearing in mind that the value of  $c_f = 1466$  m/s was assumed. This comparison also demonstrates that the method outlined in this study can be used (with a good level of accuracy) in an analysis where the fluid is assumed incompressible, simply by using (5), replacing the Laplace equation to model the velocity potential of the fluid and using a large value of speed of sound  $c_f$ .

### 2.3 Modal energy representation

In this study, since in all cases we are dealing with some degree of structural/fluid vibration interaction, it would be erroneous to describe any mode of vibration as either purely a structural mode or an acoustic (fluid) mode. For most cases the modes are either predominantly structural with acoustic interference or predominantly acoustic with structural interference. However, under certain conditions natural modes can exhibit characteristics which can be more appropriately described as *strong interacting modes* where the vibration energy is approximately equally divided between structural and fluid vibration energy. It is modes such as these which are of most interest and are the main focus of this study. In an attempt to quantify the degree of coupling and describe whether modes are mainly structural or acoustic or strongly coupled, attention will be drawn to the distribution of vibration kinetic energy between the structural and fluid components of the system.

For the membrane, the peak kinetic energy of vibration  $\text{KE}^c$  for a selected value of  $m$  is calculated from

$$\text{KE}^c = \sum_{s=1}^n \text{KE}_s^c$$

where

$$\text{KE}_s^c = \pi \rho_c h a^4 \omega^2 \int_0^1 [\chi_{m,s} \psi_{m,s}(\bar{r})]^2 \bar{r} d\bar{r} ,$$

noting that the eigenvectors  $\psi_{m,s}(\bar{r})$  are orthogonal.

For the fluid the maximum kinetic energy  $\text{KE}^f$ , for a selected value of  $m$ , is calculated from (noting orthogonality of eigenvectors describing  $\bar{\varphi}_m$ ):

$$\text{KE}^f = \sum_{q=1}^n \text{KE}_q^r + \sum_{q=1}^n \text{KE}_q^x = \text{KE}^r + \text{KE}^x$$

where

$$\text{KE}_q^r = \rho_f \pi a^2 L \int_0^1 \int_0^1 (V_q^r)^2 \bar{r} d\bar{r} d\bar{x} ,$$

$$\text{KE}_q^x = \rho_f \pi a^2 L \int_0^1 \int_0^1 (V_q^x)^2 \bar{r} d\bar{r} d\bar{x} ,$$

and by using (9) and (11)

$$V_q^r = c_f \frac{\partial \hat{\varphi}_{m,q}}{\partial \bar{r}}, \quad V_q^x = \frac{ac_f}{L} \frac{\partial \hat{\varphi}_{m,q}}{\partial \bar{x}},$$

$$\hat{\varphi}_{m,q} = B_{m,q} \cos(\gamma_{m,q}^{(\lambda)} \bar{x}) J_m(\alpha_{m,q} \bar{r}) \cos(m\theta).$$

The percentage energy associated with  $\text{KE}^f$  and  $\text{KE}^c$  are expressed as

$$\% \text{KE}^x = \frac{\text{KE}^x}{\text{KE}^f + \text{KE}^c} \times 100 \% \quad \text{for total axial fluid energy ,}$$

$$\% \text{KE}^r = \frac{\text{KE}^r}{\text{KE}^f + \text{KE}^c} \times 100 \% \quad \text{for total radial fluid energy ,}$$

$$\% \text{KE}^c = \frac{\text{KE}^c}{\text{KE}^f + \text{KE}^c} \times 100 \% \quad \text{for total membrane energy .}$$

A set of energy vectors for the membrane and fluid is defined as follows:

$$\mathbf{KE}_q^r = (\% \text{KE}_1^r, \% \text{KE}_2^r, \dots, \% \text{KE}_q^r, \dots, \% \text{KE}_n^r)$$

is the vector of radial kinetic energy components ( $q=1,2,\dots,n$ ) of the fluid,

$$\mathbf{KE}_q^x = (\% \text{KE}_1^x, \% \text{KE}_2^x, \dots, \% \text{KE}_q^x, \dots, \% \text{KE}_n^x)$$

is the vector of axial kinetic energy components ( $q=1,2,\dots,n$ ) of the fluid, and

$$\mathbf{KE}_s^c = (\% \text{KE}_1^c, \% \text{KE}_2^c, \dots, \% \text{KE}_s^c, \dots, \% \text{KE}_n^c)$$

is the vector of kinetic energy of lateral vibration components ( $s=1,2,\dots,n$ ) of the membrane where

$$\% \text{KE}_q^r = \frac{\text{KE}_q^r}{\text{KE}^f + \text{KE}^c} \times 100 \% ,$$

$$\% \text{KE}_q^x = \frac{\text{KE}_q^x}{\text{KE}^f + \text{KE}^c} \times 100 \% ,$$

$$\% \text{KE}_s^c = \frac{\text{KE}_s^c}{\text{KE}^f + \text{KE}^c} \times 100 \% .$$

For later reference, the energy ratio  $F_e(\lambda)$  is defined for a selected value of  $m$  as

$$F_e(\lambda) = \frac{\text{total energy associated with membrane}}{\text{total energy associated with fluid}} = \frac{\text{KE}^c}{\text{KE}^f} . \quad (18)$$

Consequently, having obtained the root values of  $\lambda$  and the corresponding values of mode shape coefficients  $\chi_{m,1}, \chi_{m,2}, \dots, \chi_{m,s}, \dots, \chi_{m,n}, \dots$ , the relative energy distribution between the membrane and the fluid components can be computed and used as a basis to describe the membrane/fluid coupled modal characteristics.

## 2.4 Numerical results

From (17) it is evident that only three selected parameters, namely  $\beta$ ,  $\kappa$  and  $\bar{L}$  (as contained in  $\gamma_{m,q}^{(\lambda)}$  for values of  $q > 1$ ), will determine a unique set of values of  $\lambda$ , corresponding mode shape coefficients and relative energy vectors.

To demonstrate the benefit of listing relative energy levels, consider the case of a slender fluid cavity ( $\bar{L} = 10$ ) and the mass of the membrane equal to the mass of the fluid cavity ( $\beta = 1$ ). In addition, in an attempt to induce strong interacting modes, the non-dimensionalised natural frequency of the first axisymmetric mode of the membrane in the absence of fluid interaction  $\lambda_{0,1} = \xi_{0,1} \sqrt{\kappa/\beta}$  is set equal to that of the first axial mode *only* ( $\bar{\alpha}_{0,1} = 0$ ) of the same fluid cavity with a rigid boundary replacing the membrane. In this case, from (9),  $(\partial \bar{\varphi}_m / \partial \bar{x})|_{\bar{x}=1} = 0$ , i.e.  $\gamma_{0,1}^\lambda = \pi = \lambda_{0,1} = 2.4048 \sqrt{\kappa/\beta}$ , giving  $\kappa = 1.707$ .

A general expression to describe this postulated condition for strong membrane/fluid vibration coupling would be

$$\xi_{m,s}^2 \frac{\kappa}{\beta} = (\eta\pi)^2 + \bar{\alpha}_{m,q}^2 \quad (19)$$

where  $\eta$  is the number of axial half waves in the fluid. In our specific case described above we have selected  $\eta = 1$ ,  $m = 0$ ,  $s = 1$  ( $\xi_{0,1} = 2.4048$ ) and  $m = 0$ ,  $q = 1$  ( $\bar{\alpha}_{0,1} = 0$ ). Thus only the axisymmetric modes ( $m = 0$ ) of vibration are considered.

Table 2 lists the results of this demonstration where  $n = 6$  in accordance with the convergence test outlined in Appendix. This table presents details of the first 6 coupled modes of vibration up to a non-dimensional frequency  $\lambda = 11.227$ , which is close to that corresponding to the third natural frequency of the membrane in the absence of interaction,  $\lambda_3 = 11.3028$ . From this table it is evident that the modal energy of the subsystems renders a useful and interesting means of describing the degree of coupling and dominance of the membrane or fluid. It is also interesting to note that for modes with a strong or moderate structural component, the vector of mode shape coefficients  $\chi$  is very well defined. For example for the first two strongly coupled modes (1 and 2) with frequencies around that corresponding to the first natural frequency of the membrane in the absence of fluid interaction,  $\chi = (1, \sim 0, \sim 0, \dots)^T$  and for mode 4, which is once again structurally dominant at a frequency close to that of the second natural frequency of the membrane in the absence of fluid interaction,  $\chi = (\sim 0, 1, \sim 0, \sim 0, \dots)^T$ . On the other hand, for modes of a strong acoustic nature only where very little energy is attributed to the membrane, such as mode 5 in Table 2, it is observed that the vector  $\chi$  indicates significant contributions from more than one structural mode.

Table 2. Modes of free vibration of the membrane/fluid interacting system with associated energy vectors

$\lambda$		Mode description
2.600 (mode 1)	$\chi = (1, \sim 0, \sim 0, \dots)^T$ $\mathbf{KE}_s^c = (38.71, \sim 0, \sim 0, \dots)$ $\mathbf{KE}_q^x = (61, \sim 0, \sim 0, \dots)$ $\mathbf{KE}_q^r = (\sim 0, \sim 0, \dots)$	Strongly coupled mode at $s = 1, q = 1$
3.705 (mode 2)	$\chi = (1, \sim 0, \sim 0, \dots)^T$ $\mathbf{KE}_s^c = (49.42, \sim 0, \sim 0, \dots)$ $\mathbf{KE}_q^x = (50.02, \sim 0, \sim 0, \dots)$ $\mathbf{KE}_q^r = (\sim 0, \sim 0, \sim 0, \dots)$	Strongly coupled or st/ac mode at $s = 1, q = 1$
6.338 (mode 3)	$\chi = (1, -0.207, \sim 0, \dots)^T$ $\mathbf{KE}_s^c = (0.5, \sim 0, \sim 0, \dots)$ $\mathbf{KE}_q^x = (99.5, \sim 0, \sim 0, \dots)$ $\mathbf{KE}_q^r = (\sim 0, \sim 0, \sim 0, \dots)$	Almost total fluid axial energy with small amount of structural interference, $q = 1$
7.206 (mode 4)	$\chi = (\sim 0, 1, \sim 0, \sim 0, \dots)^T$ $\mathbf{KE}_s^c = (\sim 0, 87.6, \sim 0, \dots)$ $\mathbf{KE}_q^x = (10.6, 0.5, \sim 0, \dots)$ $\mathbf{KE}_q^r = (\sim 0, \sim 0, \sim 0, \dots)$	Structural dominated mode with axial fluid interference, $s = 2, q = 1$
9.5192 (mode 5)	$\chi = (0.7, -1, -0.95, 0.23, \dots)^T$ $\mathbf{KE}_s^c = (\sim 2, \sim 2, \sim 1, \dots)$ $\mathbf{KE}_q^x = (95, \sim 0, \sim 0, \dots)$ $\mathbf{KE}_q^r = (\sim 0, \sim 0, \sim 0, \dots)$	Axial fluid dominated mode with structural interference, $q = 1$
11.227 (mode 6)	$\chi = (\sim 0, \sim 0, 1, \sim 0, \dots)^T$ $\mathbf{KE}_s^c = (\sim 0, \sim 0, 96, \dots)$ $\mathbf{KE}_q^x = (3, \sim 0, \sim 0, \sim 0, \dots)$ $\mathbf{KE}_q^r = (\sim 0, \sim 0, \sim 0, \dots)$	Structural dominated mode with axial fluid interference, $s = 3, q = 1$

### 2.5 The “bar” model approximation

The configuration investigated in Sec. 2.4 had the ratio  $\bar{L} = L/a = 10$  and thus resembles a long slender fluid column where only axial modes would prevail as shown in Table 2. Also, we proposed that a condition for strong vibration interaction between the fluid column and membrane would arise when the natural frequency of an axisymmetric mode of the membrane in the absence of fluid interaction equated to that of an axial mode of the same fluid cavity with a rigid boundary replacing the membrane. In this case we selected the first axisymmetric mode of the membrane set equal to that of the first axial mode only ( $\bar{\alpha}_{0,1} = 0$ ) of the same fluid cavity with a rigid boundary replacing the membrane. The results presented in Table 2 demonstrated this strong vibration

interaction between the fluid column and membrane at frequencies on either side of that common frequency ( $\lambda = \pi$ ). In an attempt to investigate further this same condition leading to strong vibration interaction we propose that the membrane fluid interacting system studied in this paper can be, to a point, represented by a “bar” model as shown in Fig. 2. In this model the discrete mass/spring system represents the membrane and the bar is analogous to the slender fluid column. By using such an approximate model it is assumed that only axial oscillations of the fluid column are considered and the membrane is restrained to free vibration around only one of its natural modes and not influenced by any of its other natural modes.

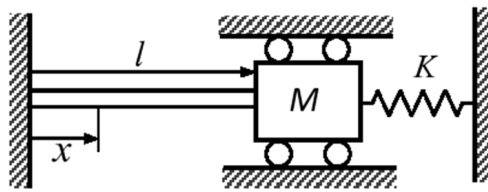


Fig. 2. The “bar” model

For the simple “bar” model (see [18]) shown in Fig. 2, it can be shown that the natural frequency roots  $\lambda$  are calculated from the equation

$$\frac{\tau}{\lambda^2} + \frac{1}{\lambda \tan \lambda} = \beta \quad (20)$$

where  $\lambda = \omega L/c_f$ ,  $L$  is length of the bar,  $c_f = \sqrt{E/\rho_f}$  is the speed of longitudinal waves in the bar,  $E$  is Young’s modulus and  $\rho_f$  is density of the bar material,

$$\begin{aligned} \tau &= \frac{K}{\text{axial stiffness of the bar}} \equiv \\ &\equiv \frac{\text{lateral axisymmetric stiffness of the membrane}}{\text{axial stiffness of fluid in cavity}} = \xi_{0,s}^2 \kappa, \end{aligned}$$

and

$$\beta = \frac{M}{\text{mass of the bar}} \equiv \frac{\text{mass of membrane}}{\text{mass of fluid in cavity}}$$

as before. Similarly, we now propose that a condition for strong vibration interaction between the bar and the discrete spring/mass system will arise when the natural frequency of the discrete spring/mass system is set equal to the natural frequency of one of the axial modes of the bar if held rigid at both ends. This can be represented by

$$(\eta\pi)^2 = \frac{\tau}{\beta}, \quad (21)$$

which is similar to (19) with  $\bar{\alpha}_{m,q}^2 = 0$ , which implies that *this model can approximate only situations comprising axial fluid modes ( $q = 1$ ) and axisymmetric fluid and membrane modes ( $m = 0$ )*. Once again  $\tau \equiv \xi_{0,s}^2 \kappa$  and  $\eta$  is the selected number of half waves present in the axial mode. Therefore combining (20) and (21) gives

$$F_{\lambda}^{\beta} = \beta \tag{22}$$

where

$$F_{\lambda}^{\beta} = \frac{1}{\lambda \tan \lambda} \frac{1}{1 - \left(\frac{\eta\pi}{\lambda}\right)^2} .$$

Also, for this simplified “bar” model we can write the corresponding energy ratio  $F_e^b(\lambda)$  (introduced in (18)) as

$$F_e^b(\lambda) = \frac{\text{vibration energy associated with } M}{\text{vibration energy associated with the bar}} = \beta \bar{F}_e^b(\lambda) \tag{23}$$

where (see [18])

$$\bar{F}_e^b(\lambda) = \frac{1 - \cos(2\lambda)}{1 - \frac{1}{2\lambda} \sin(2\lambda)} .$$

Then combining (22) and (23) gives

$$F_e^b(\lambda) = \frac{1}{\lambda \tan \lambda} \frac{1}{1 - \left(\frac{\eta\pi}{\lambda}\right)^2} \frac{1 - \cos(2\lambda)}{1 - \frac{1}{2\lambda} \sin(2\lambda)} .$$

Figure 3-*top* and Fig. 3-*bottom* are plots of functions  $F_{\lambda}^{\beta}$  and  $F_e^b(\lambda)$  to a base of  $\lambda$  for this “bar” model for the case where  $\eta = 1$  and 2, respectively, in (22). Accordingly by (22), the frequency roots are obtained from where the  $F_{\lambda}^{\beta}$  curves intercept with a horizontal line representing any value of  $\beta$  (the corresponding value of  $\tau$  is then calculated from (21)) and the relevant energy ratio is then the corresponding value of  $F_e^b(\lambda)$ . In Fig 3 the horizontal lines representing  $\beta = 1$  and  $\beta = 10$  are included. Figure 3-*top* and Fig. 3-*bottom* demonstrate that for any value of  $\beta$  the non dimensional frequencies ( $\lambda$ ) of the two strongly coupled modes will lie almost symmetrically about  $\pi$  and  $2\pi$ , respectively, and as  $\beta$  and the corresponding value of  $\tau$  from (22) increase, the frequencies of the two strongly coupled modes assume closer values around  $\pi$  and  $2\pi$ , respectively. Also of interest is the observation that the maximum value of  $F_e^b(\lambda)$  which can be obtained is approximately 1 and will always be assigned to the second of these couple modes.

For the case where  $\eta = 1$  only (interaction with the first bar/fluid axial mode), Table 3 lists the numerical values of non dimensional frequencies  $\lambda$

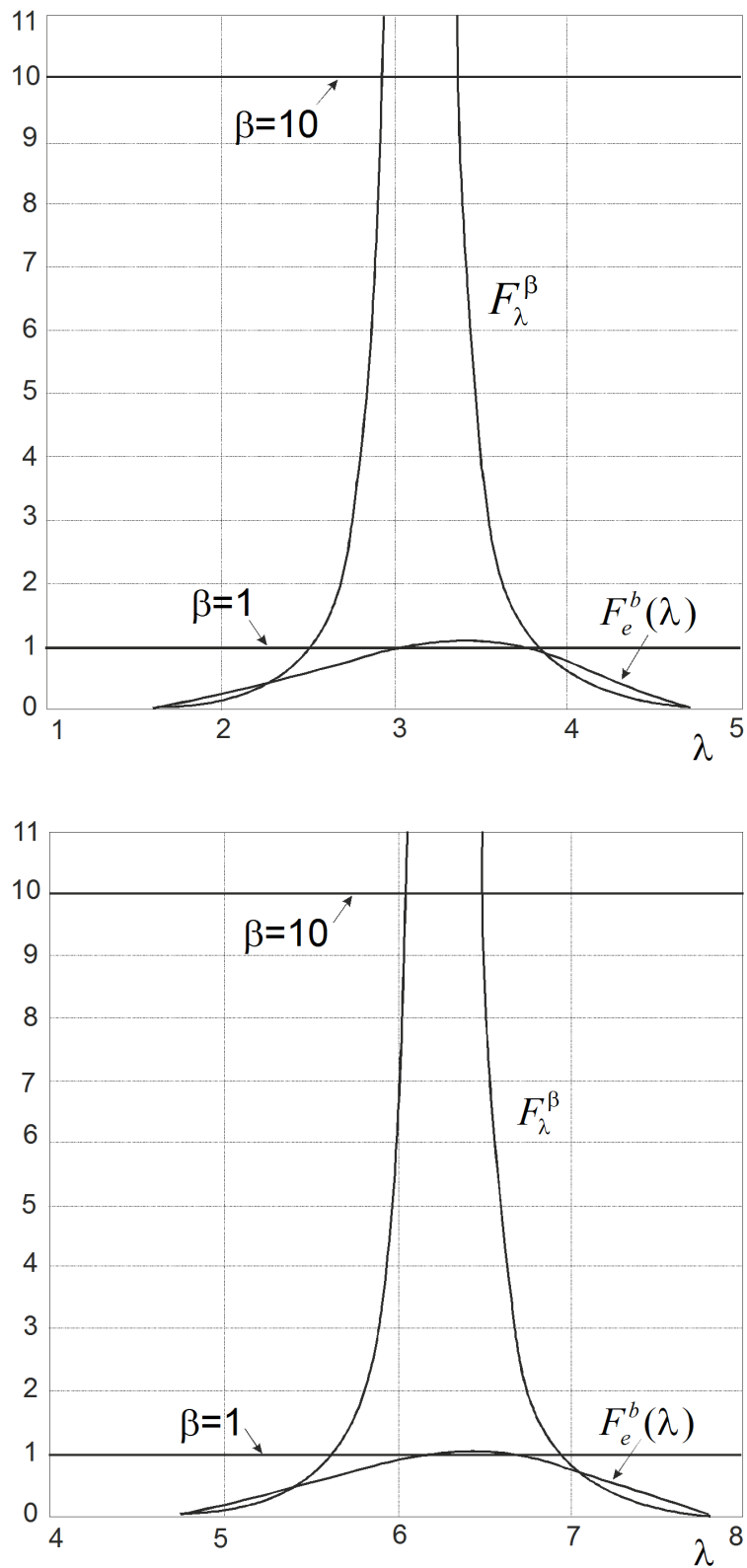


Fig. 3. Plot of  $F_\lambda^\beta$  and  $F_e^b(\lambda)$  to a base of  $\lambda$  for the “bar” model;  
*top:  $\eta = 1$ , bottom:  $\eta = 2$*

Table 3. Comparison of values of  $\lambda$  and corresponding  $\bar{F}_e(\lambda)$  obtained from the “bar” analysis (Eqs. (22) and (23)) and from the full coupled analysis (Eqs. (17) and (18))

	Root values of $\lambda$ from (22) for the “bar” model	Root values of $\lambda$ from (17) for the complete coupled model		Corresponding values of $F_e^b(\lambda)$ from (23) for the root values of $\lambda$ from (22) for the “bar” model	Values of $F_e(\lambda)$ from (18) for the root values of $\lambda$ from (17) for the complete coupled model	
		$\bar{L} = 10$	$\bar{L} = 5$		$\bar{L} = 10$	$\bar{L} = 5$
$\tau \equiv \xi_{0,s}^2 \kappa = 9.872$ $\beta = 1$	2.520	2.600	2.597	0.571	0.633	0.653
	3.821	3.705	3.697			
$\tau \equiv \xi_{0,s}^2 \kappa = 98.72$ $\beta = 10$	2.924	2.958	2.958	0.871	0.895	0.938
	3.367	3.329	3.328			

of these strongly coupled modes for the pair ( $\beta = 1, \tau = 9.872$ ) and the corresponding values of  $F_e^b(\lambda)$  for the “bar” model (solved from (20) and (21)). This table also compares them to corresponding values of  $\lambda$  and  $F_e(\lambda)$  obtained from the full comprehensive analysis, i.e., from the solution of (17) and (18) using ( $\beta = 1, \tau \equiv \xi_{0,s}^2 \kappa = 9.872$ ) for  $\bar{L} = 10, 5, 2$ . Similarly, this table list the corresponding values obtained for the parameters ( $\beta = 10, \tau \equiv \xi_{0,s}^2 \kappa = 98.72$ ).

Table 3 shows that the simple “bar” model produces root values of  $\lambda$  which are reasonably close to the values obtained from the completely coupled analysis (compare the first two columns) and corresponding values of  $F_e^b(\lambda)$  which are of the same order as those from the completely coupled analysis. The reason for these differences in numerical results is that the “bar” model, represented by (22) and (23), neglects the influence of both radial fluid modes and contributions from other membrane modes and should therefore not be used for the purpose of obtaining exact values. However the “bar” model plots of Fig. 3 are useful in that they give a visual representation of the general influence of the pairs ( $\beta, \tau \equiv \xi_{0,s}^2 \kappa$ ) on the characteristics of the natural roots  $\lambda$  of these strongly coupled modes and corresponding values of energy ratio.

### 3. Conclusions

The analysis presented in this paper was primarily related to membrane interaction with compressible fluids. However it has been shown that when applied to a case involving interaction with an incompressible fluid it produced results, which compared favourably with the analysis of another study. Also, from the analysis and results presented it has been shown that the introduction and use of modal energy of the membrane/fluid subsystems renders a useful and interesting means of describing the degree of coupling and dominance of the membrane or fluid. In this paper a simple “bar” model was used to represent a strong membrane/fluid interacting vibrating system. Whilst not producing results of sufficient accuracy compared to those of the coupled and rigorous analysis of the membrane/fluid system, it did however present a good insight into the effect of the system parameters upon the overall characteristics of the interacting system.

### Appendix: Convergence

Table A lists the first two values of  $\lambda$  obtained for  $n = 2, 4, 6, 8$  ( $n$  denoting the order of the matrix  $\mathbf{A}$  in (15)),  $\beta = 1, \kappa = 1.707, \bar{L} = 10$ .

From Table A, it is seen that convergence is extremely fast with respect to  $n$ ; requiring only  $n = 6$  for a fully converged result to 3 decimal places for these lower modes. Accordingly, forthwith  $n = 6$  will be used throughout.

Table A. Convergence

$n = 2$	$n = 4$	$n = 6$	$n = 8$
2.5829	2.597	2.600	2.600
3.7219	3.708	3.705	3.705

## References

- [1] E. H. DOWELL, G. F. GORMAN, D. A. SMITH: *Acoustoelasticity: General theory, acoustic natural modes and forced response to sinusoidal excitation, including comparisons with experiment*. J. Sound and Vibration 52 (1977), 519–542.
- [2] F. FAHY: *Sound and Structural Vibration*. Academic Press, London 1993.
- [3] Š. MARKUŠ, T. NANASI, O. ŠIMKOVÁ: *Vibroakustika zakrytykh polosteĭ* (Vibroacoustics of enclosed cavities). Dinamika tel, vzaimodeĭstvuyushchikh so sredoi (A. N. Guz et al., Eds.), Naukova dumka, Kiev 1991.
- [4] J. PRETLOVE: *Free vibrations of a rectangular panel backed by a closed rectangular cavity*. J. Sound and Vibration 2 (1965), 197–209.
- [5] J. PAN, D. A. BIES: *The effect of fluid-structural coupling on sound waves in an enclosure—Experimental part*. J. Acoust. Soc. Am. 87 (1990), 708–721.
- [6] V. B. BOKIL, U. S. SHIRAHATTI: *A technique for the modal analysis of sound-structure interaction problems*. J. Sound and Vibration 173 (1994) 23–41.
- [7] M. R. LEE, R. SINGH: *Analytical formulations for annular disk sound radiation using structural modes*. J. Acoust. Soc. Am. 95 (1994), 3311–3313.
- [8] D. G. GORMAN, J. M. REESE, J. HORACEK, K. DEDOUCH: *Vibration analysis of a circular disc backed by a cylindrical cavity*. Proc. Instit. Mech. Engineers, Part C 215 (2001), 1303–1311.
- [9] D. G. GORMAN, I. TRENDAFILOVA, A. J. MULHOLLAND, J. HORÁČEK: *Vibration analysis of a circular plate in interaction with an acoustic cavity leading to extraction of structural modal parameters*. Thin-Walled Structures 46 (2008), 878–886.
- [10] H. F. BAUERAND, M. CHIBA: *Hydroelastic viscous oscillations in a circular cylindrical container with an elastic cover*. J. Fluids Struct. 14 (2000), 917–936.
- [11] M. AMABILI, G. FROSALI, M. K. KWAK: *Free vibrations of annular plates coupled with fluids*. J. Sound and Vibration 191 (1996), 825–846.
- [12] M. AMABILI: *Effect of finite fluid depth on the hydroelastic vibrations of circular and annular plates*. J. Sound and Vibration 193 (1996), 909–925.
- [13] C. RAJALINGHAM, R. B. BHAT, G. D. XISTRIS: *Vibration of circular membrane backed by cylindrical cavity*. Int. J. Mech. Sci. 40 (1998), 723–734.
- [14] S. TARIVERDILO, J. MIRZAPOUR, M. SHAHMARDANI, G. REZAZADEH: *Free vibration of membrane/bounded incompressible fluid*. Appl. Math. Mech. 33 (2012), 1167–1178.
- [15] A. W. LEISSA: *Vibration of plates*. NASA SP-160, Washington 1969.
- [16] E. KREYSZIG: *Advanced engineering mathematics*. 9th Ed., Wiley 2006.
- [17] N. W. MCLACHLAN: *Bessel functions for engineers*. Oxford Univ. Press, London 1948.
- [18] S. S. RAO: *Mechanical vibrations*. 4th Ed., Pearson Education International 2004.